Microwave Journal

A Planetary Radar System for Detection and High-Resolution Imaging of Nearby Celestial Bodies

Steven R. Wilkinson, Charlie Hansen, Barry Alexia, Bishara Shamee and Brian Lloyd
Raytheon Intelligence & Space, El Segundo, Calif.

Anthony Beasley and Walter Brisken
National Radio Astronomy Observatory, Charlottesville, Va.

Flora Paganelli, Galen Watts and Karen O'Neil
Green Bank Observatory, W. Va.

Patrick Courtney
Qorvo, Richardson, Texas

In partnership with National Radio Astronomy Observatory (NRAO) and Raytheon Intelligence & Space (RI&S), the Green Bank Observatory (GBO) tested a multi-static radar intended to expand the scientific reach and capability of the Green Bank Telescope (GBT) and the Very Long Baseline Array (VLBA). The experimental effort installed an RI&S Ku-Band transmitter on the GBT and relied on VLBA receiving stations to receive the data transmission. That transmission generated synthetic aperture radar (SAR) images of select locations on the moon and detected asteroid 2001 FO32.

Radio astronomers have long been seeking to expand the capabilities of radar in their observations of the Solar System. In early 2019, efforts were initiated at the GBO GBT and the NRAO's VLBA to accomplish this expansion. Following the collapse of the 300 m Arecibo Telescope in December 2020, the astronomy community raised questions about the future of some types of work conducted there, including the use of planetary radar systems for the observation of asteroids, inner- and outer-Solar System bodies and moons. The GBT and VLBA can expand on this work using an active radar system for planetary radar applications. Tests of this capability resulted in successful experimental efforts toward ground-based high-resolution imaging of nearby celestial bodies.

SYSTEM DESIGN

Selection of the GBT transmission frequency was interesting since NRAO discussions centered on Ka-Band. The experiment planned to use the VLBA as a receiver, but the array did not have a Ka-Band receiver like NRAO's Very Large Array. Review of the VLBA receiving bands focused on the highest frequencies below Ka-Band possible. Analysis determined the best frequencies were from 13.75 to 14.0 GHz. The final license covered a 200 MHz bandwidth from 13.8 to 14.0 GHz.

The transmitter was installed on the GBT at the prime focus (PF) position. It was developed to be compatible with existing GBT interfaces, and to be controlled and monitored remotely via a secure internet link. A duplexer allowed

Reprinted with permission of MICROWAVE JOURNAL® from the January 2022 issue.
©2022 Horizon House Publications, Inc.

TABLE 1

GBT TRANSMITTER SPECIFICATIONS

Parameter	Value
Transmitter Output Power	650 W
Transmitter Frequency	13.9 GHz
Maximum Transmit Bandwidth	200 MHz
Receiver Bandwidth	11.0–12.8 GHz
Transmitter-Receiver Isolation	> 85 dB

the transmitter and a pointing receiver to be connected to the same feed horn. The system was either in transmit or receive mode. Specifications for the transmitter and pointing receiver are listed in ***Table 1***.

The GBO uses standard receiver housings for installation at the PF of all large antennas on site. For ease of installation and removal, the RI&S Ku-Band transmitter was built inside one of these PF housings (PFH). The housing consists of a rectangular box approximately 28 × 28 × 60 $in.^3$ with brackets for hoisting and attaching to the mounting cage at the antenna focus. One 28 × 28 in. panel of the box carries the feed horn, while the opposite 28 × 28 in. panel carries connectors and fittings for the RF, electrical and cooling connections. The receiver mounting cage can be moved small distances in the X- and Y-directions parallel to the primary reflector, moved toward or away from the primary reflector to change receiver focus and rotated in both directions around the receiver axis.

In November 2019, GBO shipped the PFH to RI&S for transmitter installation. The Peltier coolers were removed and replaced with a simple ethylene/glycol heat exchanger. The system block diagram is shown in ***Figure 1***. The blocks in the light gray background were integrated into the PFH. Testing included verification of the gate biasing, power sequencing and pulse testing of the power supply into 5000 W loads. Mechanical members were water-jet-cut from aluminum slabs to ensure structural integrity, weight and balance. The payload needed to remain stable while being lifted and stowed into position atop the 500-ft. telescope. Pre-installation transmission tests occurred in GBO laboratories. The RI&S transmitter (see ***Figure 2***) operated at full power into an RF load, which verified both the transmitter status and remote operations.

TRANSMITTER DEVELOPMENT

The aggressive schedule and budget constraints mandated the use of commercial off-the-shelf hardware. RI&S conducted a detailed survey of high-power microwave amplifiers that included solid-state, TWTs, magnetrons, klystrons and cross field amplifiers. Size, weight, power and cost requirements and the need for continuous wave (CW) operation quickly narrowed the field. The Qorvo Spatium power amplifier was the only option that met these requirements. Graceful degradation, an integrated bias and sequencing, connectorized cooling jacket and simple 28 VDC power requirement in a compact volume made the Spatium the only choice (see ***Figure 3***). The Spatium output power and VLBA sensitivity enabled the capability to generate spectacular lunar SAR images.

The Spatium amplifier is composed of an antipodal finline antenna array that is loaded into a coaxial waveguide to create a broadband multi-element combiner structure. The Spatium structure has demonstrated performance from 2 to 40 GHz and up to a decade of bandwidth in an individual amplifier. Qorvo has released a line of standard products based on the Spatium technology that is broken into three platforms covering typical radar, jammer and communications transmitter bands: 2 to 20 GHz, 8 to 16 GHz and 18 to 40

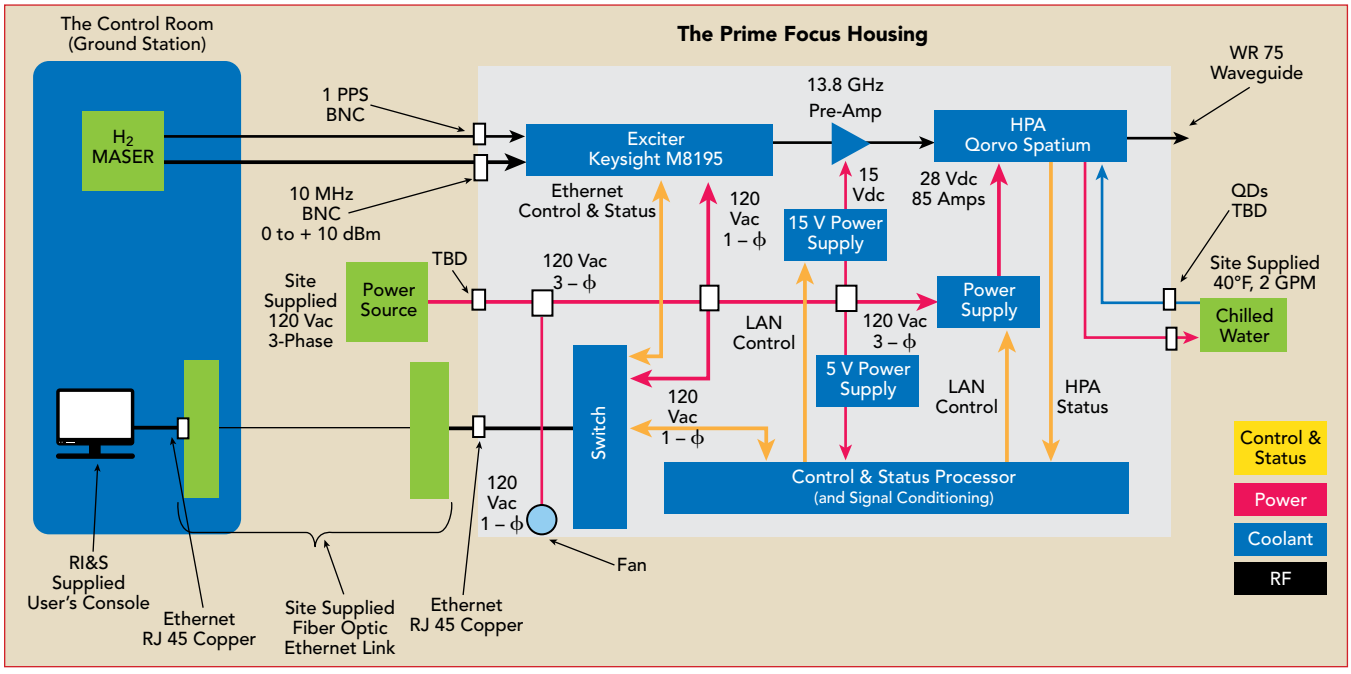

Fig. 1 **System block diagram.**

Fig. 2 **RI&S transmitter.**

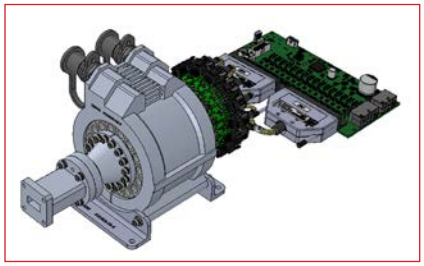

Fig. 3 **Spatium power amplifier.**

GHz. Each of the standard Spatium platforms allows for the combining of 16 solid-state amplifiers.

The Qorvo QPB1316 power amplifier uses the 8 to 16 GHz standard Spatium platform, combining 16 solid-state GaN MMIC amplifiers to achieve greater than 500 W of CW output power with a typical power-added efficiency of 27 percent. This high power amplifier (HPA) is compact with outline dimensions of 4.15 × 5.28 × 9.4 in., and with 3.35 × 6.89 in. for the associated bias control printed circuit board assembly (PCBA). Included in the dimensions is an integrated liquid-cooled clamp that allows the HPA to operate in both pulsed and CW modes while minimizing thermal resistance from the system cooling fluid to the GaN MMIC devices. The bias control PCBA requires a +28 VDC input and contains all required gate voltage and sequencing circuitry required for the GaN MMIC devices along with current monitoring for each of the 16 devices within the Spatium amplifier. The bias control PCBA is standard with Spatium products to ease integration at the next highest assembly transmitter.

TRANSMITTER INTEGRATION AND TEST

Figure 4 is an overall block diagram of the transmitter identifying the GBT interfaces to include power, coolant, references, control communications and RF transmission. The control communications channel is a fiber channel to support a remote distance of 3.1 km between the local control node and the GBT. The operator control node is a remote internet node that was not originally planned but designed into the system to mitigate COVID-19 travel constraints.

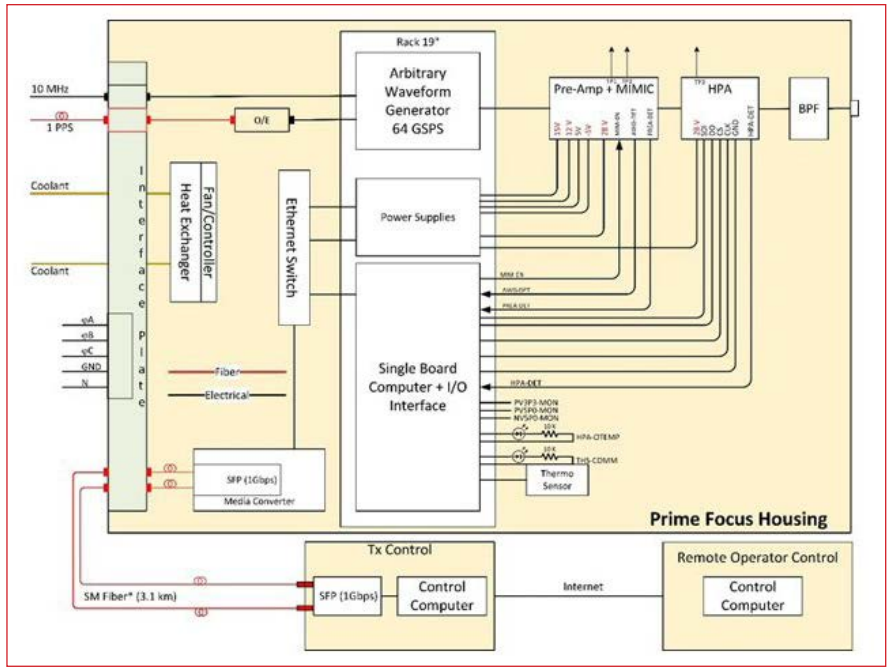

Fig. 4 **Transmitter block diagram.**

Ultimately, the internet became the only way to operate the transmitter. The transmitters critical elements are the HPA driven by an arbitrary waveform generator (AWG) running at 64 giga samples per second with eight bits of precision. The AWG synthesizes the tones and the linear frequency modulated (LFM) waveforms at the center frequency of 13.9 GHz without upconversion to reduce hardware and additional impairments. The preamplifier is enabled to drive the HPA with the synthesized waveform and the state vector is constantly monitored until a new waveform is required, or the test is terminated, by disabling transmission and shutting down gracefully. The flow diagram is depicted in ***Figure 5***.

During pre-installation GBO testing, all potential waveforms and transmission periods were tested at full power with a termination and monitoring coupler in place of the feed to verify system robustness under typical use. Measurement of the 200 MHz waveform is shown in ***Figure 6***.

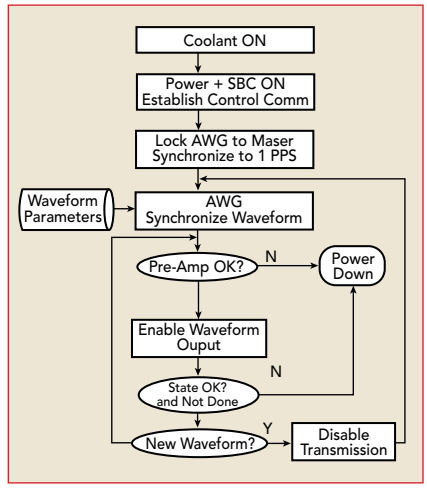

Fig. 5 **Transmitter operation.**

GBT TRANSMISSION TESTING AND CALIBRATION

Prior to the use of the GBT for transmitting, the GBT software pointing model for the PF was only accurate below 2 GHz. Without updating the software pointing model, the errors when used at 11 to 14 GHz at the PF could have been large enough for the transmitter beam to miss the target. By duplexing a pointing receiver with the transmitter using the same feed horn, on-the-fly updates of the GBT software pointing model were possible without the laborious, time-

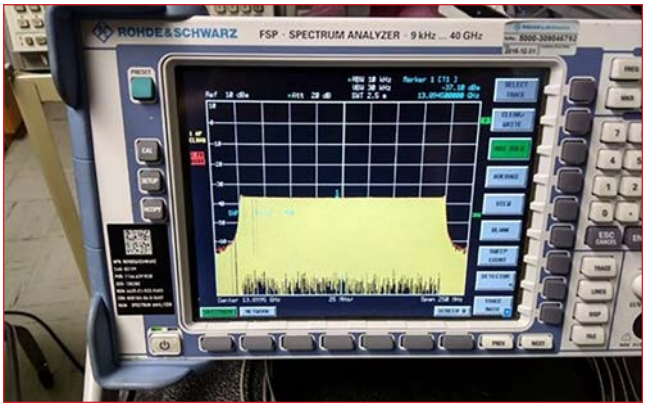

Fig. 6 **200 MHz waveform.**

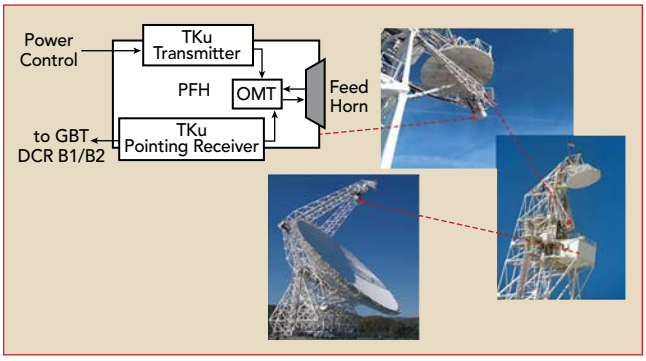

Fig. 7 **PFH block diagram and location on the GBT.**

TABLE 2

VLBA RECEIVER SPECIFICATIONS

Parameter	Value	Notes
Receive Antennas	10	All VLBA Antennas, Subject to Elevation Limits
Antenna Aperture Diameter	25 m	
System Temperature	60 K	Typical Zenith Value
Center Frequency	13.932 GHz	
Receive Bandwidth	128 MHz	

consuming and potential error-inducing exchanges of the transmitter with a receiver. A general diagram of the PFH and its location on the GBT is shown in ***Figure 7***.

To enable observations with the transmitter, dedicated software changes of the GBT's Manager and Control System were needed. These changes were two-fold: 1) to enable pointing and focusing of the PF receiver; and 2) to enable the 12 GHz during the observations. Implementation of software routines allowed, within ASTRID scripts (GBT Observing Guide, 2017), pointing the transmitter using the PF at 12 GHz (rest frequency center at 11.95 GHz) to peak and focus using the GBT FITS Monitor (GFM) software.

The GFM software fits a beam pattern to a cross-scan on a calibrator and calculates the pointing offset and correction for the observations. The routines were: 1) a new configuration of the transmitter pointing receiver at the PF, rest frequency at 11.95 GHz, connected to the Digital Continuum Receiver (DCR) back-end; 2) running the pointing model at the PF; 3) GFM peak and focus interactive correction using the transmitter pointing receiver at the PF. Prior to transmissions a "pointing run" was executed, where the GBT was pointed at a Ku-Band quasar of well-known location and intensity (ranging 1 to 20 Jansky), and the antenna was moved in azimuth, then elevation. The total power detected in the pointing receiver versus azimuth and elevation directions was measured at a fine scale and from these measurements the pointing model was updated. A focus scan was then executed on the source to calibrate the focus prior to tracking using the ephemeris of the selected target and begin transmission of observations.

Transmission testing consisted of a commissioning phase in which the transmitter went through a series of warm-up cycles through transmission of specific modes of operation including CW and LFM waveforms. The VLBA receiving stations were not involved during the commissioning phase. After the transmit session, tests were dedicated to checking the receiver for pointing and focus corrections/calibration repeatability using geostationary (GEO) satellite Ku-Band beacons, i.e. GALAXY18 (GEO Slot#123.0; NORAD#32951, Az 236.5, El 27.1), and radio-astronomical calibrators (Ku-Band quasar). The transmitter was not operating during the cali-

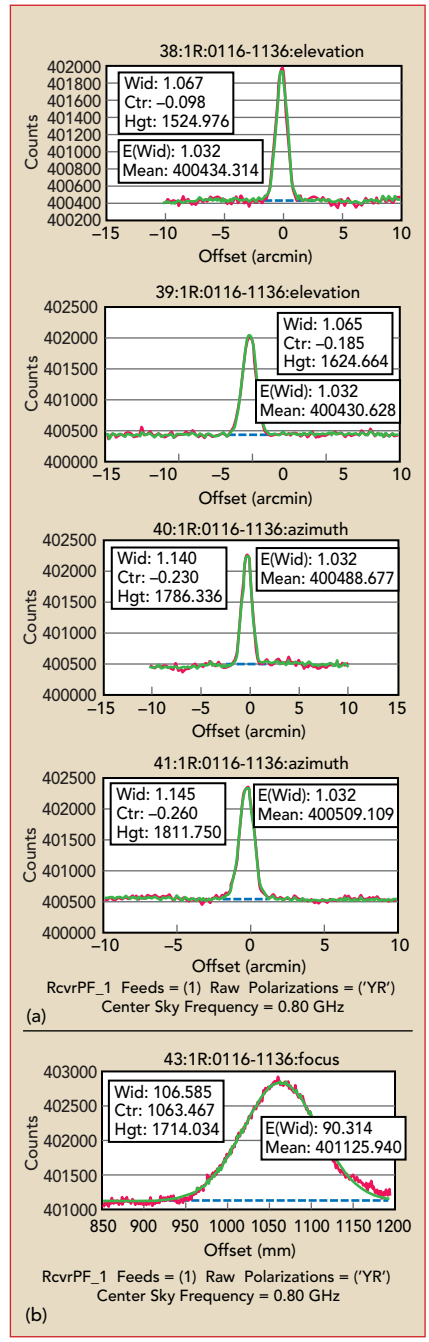

Fig. 8 **Peak (a) and focus (b) scans of the Ku-Band quasar calibrator 0116-1136 (1.151 Jy). GFM fits: baseline = dashed blue line; observation data = red; Gaussian fit = green.**

bration session.

Pointing checks were run through a series of peak scans to test the receiver's sensitivity. The artificial Ku-Band sources saturated the receiver's high-sensitivity channel but were observable switching to the low sensitivity DCR channel B1, X polarization. The radio-astronomical calibrators were observable with the receiver's high-sensitivity DCR channel B2, Y polarization. This configuration was used as default configuration for pointing, focus scans and tracking on targets for observations during transmission and data collection.

DATA COLLECTION

The observations and data collection were coordinated between the GBT and VLBA through planned observations blocks with detailed time sequence, transmit and receive parameters. Target range and elevation above the horizon with respect to transmit and receive sites was based on ephemerides derived from JPL's Horizons system.[3] The GBT operated the transmitter from an elevation between 10 and 80 degrees. The VLBA participated as a set of 10 single-dish receiving stations (see ***Table 2***).

The VLBA's back-end system and recorder were used to acquire the data. Baseband signals were recorded at a Nyquist rate for 16, 32, 128 and 256 MHz bandwidths in both circular polarizations. Data were stored in the VLBI Data Interchange Format with two bits per sample quantization. A portion of the data acquired at 16 and 32 MHz bandwidths was transferred in real time to computers at the VLBA operations center for rapid diagnostic evaluation. The complete set of recordings was later shipped on hard disk from each site. The wide geographic distribution of VLBA antennas meant that, at times, not all antennas were able to participate in the full duration of the observations.

The repeatability of performing blind pointing on preferred targets was satisfactory within a fraction of a beamwidth in azimuth and elevation depending on the sources (20 to 30 arcseconds). Focus offset was established at approximately 1050 mm (900 mm fix correction as per MRQ1R2 +150 mm adjustment), which was added as the default starting correction for the observations. These values were established during the radar run in November 2020 and confirmed in the second radar observation run in March 2021. For the Apollo 15 observation (March 13, 2021) peak and focus scans of the Ku-Band quasar calibrator 0116-1136 (1.151 Jy) are shown in ***Figure 8***, nearby the moon, before tracking on the targeted moon location. Peak scans 38 through 41 on source 0116-1136 are shown in Figure 8a. Focus scan 43 on source 0116-1136 is shown in Figure 8b. During observations, the transmission waveforms and VLBA receive modes would vary depending on observation goals. A summary of used parameters is shown in ***Table 3***.

The opportunity to observe asteroid 2001 FO32 (231937) at a close approach range of 0.01348 AU on March 21, 2021 was planned. The predicted angular difference between transmit and receive ephemeris using JPL's Horizons was 52 arcsec. Therefore, given our 54 arcsec. beamwidth, this ephemeris error required leading the target (courtesy of John Giorgini, JPL) to maximize

TABLE 3 *Ku-BAND TRANSMISSION WAVEFORMS AND VLBA RECEIVE MODES*

Transmission Waveform Parameters (AWG)								*Receive Mode*
Code	*Description*	*WF Name*	*PRI (µs)*	*BW (MHz)*	*Frequency (GHz)*	*Unambiguous Range (km)*	*Range Resolution (km)*	*VLBA Baseband (MHz)*
W00	Single Tone	LFM00	CW	0	13.9	Infinite	None	U16
W01	Asteroid Detection	LFM01	800	0.05	13.9	120	3.00	U16
W02	Asteroid Detection	LFM02	800	0.085	13.9	120	1.76	U16
W03	Asteroid Detection	LFM03	800	0.1	13.9	120	1.50	U16
W06	Asteroid Detection	LFM06	400	0.14	13.9	60	1.07	U16
W08	Asteroid Detection	LFM08	400	0.4	13.9	60	0.375	U16
W13	Asteroid Imaging	LFM13	200	1.5	13.9	30	0.100	U16
W15	Asteroid Imaging	LFM15	200	3	13.9	30	0.050	U16
W16	Ambiguity Resolution for Lunar Imaging	LFM16	2000	3	13.9	300	0.050	U16
W17	Lunar Course Imaging	LFM17	800	3	13.9	120	0.050	U16
W19	Asteroid Hi-Res Imaging	LFM19	200	6	13.9	30	0.025	U16
W20	Asteroid Hi-Res Imaging	LFM20	100	10	13.9	150	0.015	U16
W21	Asteroid Hi-Res Imaging	LFM21	100	15	13.9	15	0.010	U16
W22	Ambiguity Resolution, Lunar Medium-Res	LFM22	2000	30	13.9	300	0.005	U32
W24	Near Earth Object Imaging	LFM24	30	30	13.9	450	0.005	U32
W26	Hi-Res Lunar Imaging	LFM25	2000	120	13.932	300	0.00125	U128

Fig. 9 **Control panel while tracking FO32.**

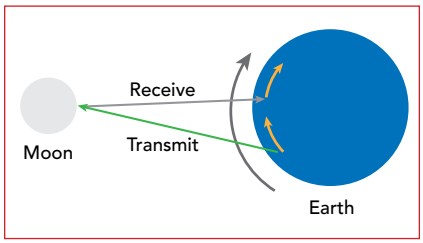

Fig. 10 **Earth-moon geometry.**

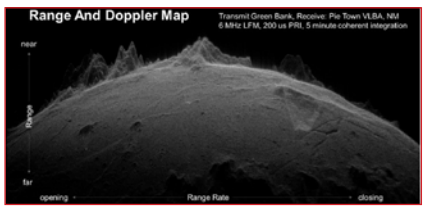

Fig. 11 **Image of the moon's surface.**

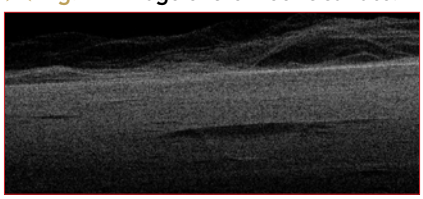

Fig. 12 **Closer view of the moon showing the inside of a crater in the foreground.**

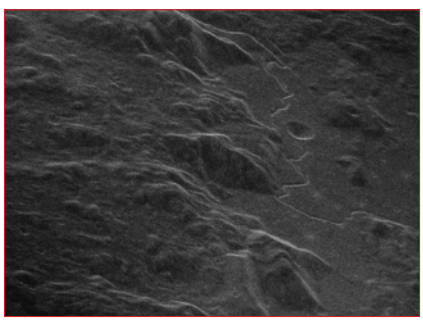

Fig. 13 **Apollo 15 landing site at 50 x 50 m resolution.**

return SNR. A control panel snapshot during tracking of FO32 and waveform transition detected at the DCR (total power counts) is shown in ***Figure 9***.

The GBT transmission experiments gave the NRAO and RI&S an opportunity to investigate ways to process long-range radar data collected that included lunar SAR imaging and detection of 2001 FO32. The moon is a perfect candidate for such tests as it is an extremely useful radar calibration target. During the March 2021 testing period, we had an opportunity to observe asteroid 2001 FO32 as well, since it approached within 5.25 lunar distances.

Moon Observations

Consider the geometry in ***Figure 10***. Because the Earth is rotating and the moon is moving in its orbit, the Doppler shifts vary as a function of position that scatter radar energy on the moon. In addition, since the linear frequency modulation on the radar signal has a defined, single-peaked autocorrelation function, processing can separate the radar return in range and range rate. Range corresponds to distance from Earth and range rate corresponds to the east-west position on the moon.

In ***Figure 11***, the vertical extent corresponds to about 25 km, while the horizontal extent corresponds to over 100 km, meaning the curvature is highly exaggerated. A closer view is shown in ***Figure 12***. Note that the inside of the crater in the foreground is visible. This is due to the mismatch between the radar geometry and the observer perspective. From the perspective of the image, the radar energy comes from the top, and illuminates everything in its direct line-of-sight, including the inside of the crater. This is a common phenomenon in radar images since every point in the radar's line-of-sight appears at a location in the image depending only on that point's range and range rate. Because of this, the horizontal axis in the image corresponds to east and west on the moon, and the vertical axis corresponds to distance toward Earth; it is impossible to know if the image shows the north or south face of the mountains in the background. It may be showing both simultaneously.

When imaging regions of the moon away from the equator, the synthetic aperture created by the rotation of Earth can be exploited to form images. During a five-minute SAR collection, the GBT moves approximately 109 km. Using digital processing, an image can be formed equivalent to a real aperture of that size. The Apollo 15 landing site, shown in ***Figure 13***, has a resolution of 50 x 50 m. With a longer dwell (40 minutes) and higher-bandwidth waveforms, higher resolution images can be formed, as shown in ***Figure 14*** (Apollo 15 with a 5 × 5 m resolution). These images were processed using the Polar Format Algorithm (PFA).[1] The PFA extends the available image size over Doppler-Delay processing, but itself has limitations on image size. Fortunately, correction algorithms are now available that enable larger and higher resolution images.

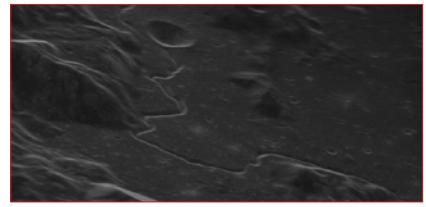

Fig. 14 **Apollo 15 landing site at 5 x 5 m resolution.**

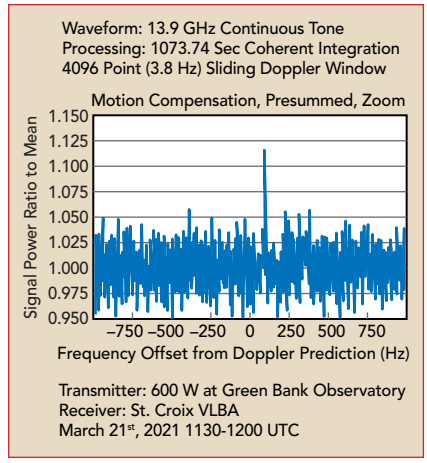

Fig. 15 **Doppler spectrum of the return from FO32 during the asteroid's close approach.**

Asteroid 2001 FO32 Observations

During the asteroid close approach, the NRAO/RI&S team tested the Ku-Band transmitter with a variety of waveforms. ***Figure 15*** shows the Doppler spectrum of the return from FO32 during one portion of this test. Because the asteroid has a large line-of-sight acceleration as it crosses Earth's orbit, its Doppler shift is changing too rap-

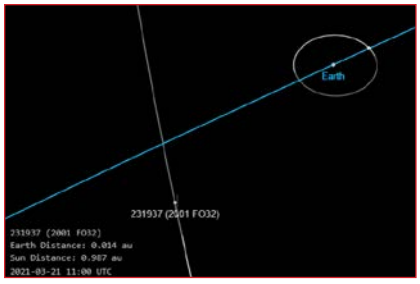

Fig. 16 Geometry of FO32's closest approach to Earth.

idly for coherent integration based on an uncompensated Doppler spectrum. ***Figure 16*** shows the geometry of the closest approach.[2]

At the closest approach, the relative range closure is zero. At five hours before the closest approach, the range rate was—10.3 km/sec (the total magnitude of velocity was 34 km/s.) Therefore at five hours before closest approach, the Doppler at a carrier frequency of 13.9 GHz was approximately 1 MHz and the rate of change of Doppler was roughly 50 Hz/sec.

Using the JPL Horizons tool,[3] a fine-grained prediction of range rate was obtained and applied as a phase to the radar return before coherent integration. The result shows a peak within 100 Hz of the expected location. In a future planetary radar system, this extremely precise measurement could be used to update the orbital ephemeris of the object in real time.

CONCLUSION

The NRAO/RI&S/Qorvo experiments demonstrated the feasibility of GBT as a transmitter to enable radar observations while testing the potential of solid-state microwave technology. The data collected during these experiments using basic radar signal processing algorithms validates the feasibility of an NRAO radar using the GBT as a transmitter and the VLBA antennas as receivers. This points the way to a future, more capable planetary radar system that can provide precision orbit determination and high-resolution images of solar system objects. It has opened the path to a new development for planetary radar capabilities at the GBT that could lead to an effective radar instrument being planned and deployed in the coming years. Microwave technical capabilities are evolving where consideration of future high-power, multiple-frequency phased array systems could provide opportunities to bridge the gap of current radar systems for solar system exploration and more. ■

ACKNOWLEDGMENTS

The authors acknowledge Frank Ghigo (GBO retiree) for his dedication and guidance through the development, testing and observations phases conducted with the GBT Ku-Band transmission experiments. Associated Universities, Inc. operates both GBO and NRAO under a cooperative agreement with NSF.

References

1. W. G. Carrara, R. S. Goodman and R. M. Majewski, "Spotlight Synthetic Aperture Radar Signal Processing Algorithms," *Artech House*, 1995.
2. Small-Body Database Lookup, Web, https://ssd.jpl.nasa.gov/sbdb.cgi?sstr=231937;orb=1;cov=0;log=0;cad=0#orb.
3. Horizons Web Application, Web, https://ssd.jpl.nasa.gov/horizons.cgi.